SPEKTA
(Jurnal Pengabdian Kepada Masyarakat: Teknologi dan Aplikasi)
ISSN 2723-8016 (online) | 2723-8008 (print)
Vol 6, No. 1, pp. 181-194

Predictive Modeling of Porosity in Al_2O_3–TiO_2 Ceramic Coatings Produced by Plasma Spraying

Duong Vu [1*], Ha Minh Hung [2]
[1] School of Engineering and Technology, Duy Tan University, Da Nang, Vietnam
[2] National Research Institute of Mechanical Engineering, Hanoi, Vietnam
*Corresponding Author: duongvuaustralia@gmail.com

ARTICLE INFO

Article history
Received October 24, 2023
Revised June 10, 2023
Accepted June 16, 2025

Keywords
Plasma Spraying;
Alloy Ceramic;
Powder Al_2O_3 – TiO_2;
Orthogonal Experiment Plan;
Metallographic Porosity.

ABSTRACT

Background: Plasma spraying is a proven technique for applying ceramic coatings to enhance the mechanical and chemical resistance of components exposed to abrasive and corrosive environments. However, controlling coating porosity remains a critical factor that directly affects the coating's performance and lifespan.
Contribution: This study contributes to the field by developing a predictive model that quantifies the influence of key plasma spraying parameters on the porosity of Al_2O_3–TiO_2 coatings. The model enables process optimization and quality control for applications requiring high-performance surface protection.
Method: An orthogonal experimental design (N27) was implemented to systematically vary three process parameters: spray distance (Lp), plasma current intensity (Ip), and powder feed rate (Gp). A total of 27 coating samples were produced and analyzed.
Results: The resulting porosity ranged from 5.96% to 14.52% depending on parameter combinations. The developed second-order polynomial regression model demonstrated good predictive accuracy, with deviation between measured and predicted values ranging from −8.67% to +13.96%, and typically within acceptable engineering limits.
Conclusion: The findings confirm that process parameters significantly affect coating porosity, and that the proposed model is a useful tool for optimizing plasma spray operations.

1. Introduction

Plasma spraying technology is widely utilized in industrial applications to enhance the surface properties of structural components, especially in environments exposed to high

mechanical stress, thermal shock, and corrosive media [1]–[3]. Among various coating materials, the Al_2O_3–TiO_2 ceramic composite stands out due to its excellent hardness, thermal stability, and corrosion resistance, making it a prime candidate for protective coatings in the aerospace, automotive, and manufacturing sectors. One of the critical performance indicators of such ceramic coatings is porosity, as it significantly affects the coating's mechanical strength, thermal conductivity, adhesion to the substrate, and overall durability under service conditions [4], [5].

However, controlling and predicting porosity in plasma-sprayed coatings remains a substantial challenge due to the complex and highly nonlinear interaction between multiple processing parameters [2], [5]. Variables such as the spray distance (Lp), plasma arc current (Ip), and powder feed rate (Gp) must be precisely calibrated, yet existing studies often report inconsistent findings or lack sufficient statistical robustness. Many prior investigations rely on trial-and-error methods or single-variable adjustments, which are inadequate for capturing the multidimensional nature of the spraying process. This gap in both theoretical modeling and practical optimization hinders the broader application and scalability of plasma spray coatings in critical engineering systems [6], [7].

In particular, while some research has examined the influence of individual parameters on coating structure, few have integrated orthogonal experimental planning to systematically evaluate their combined effects [8]. Furthermore, limited attention has been given to constructing empirical models that correlate spray parameters with porosity as a quantifiable quality index [9], [10]. As a result, there is insufficient predictive capability to support parameter selection for targeted porosity levels, especially when transitioning from laboratory-scale experiments to industrial-scale implementations [11], [12].

To address these limitations, the present study aims to investigate the relationship between key plasma spraying parameters and the resulting porosity of coatings formed from a standardized Al_2O_3–40%TiO_2 ceramic powder on SS400 carbon steel substrates. The research utilizes an extended orthogonal experimental design ($N=3^3=27$), allowing for a systematic and comprehensive exploration of the parameter space [13], [14]. Advanced image analysis techniques on metallographic samples using the Axiovert 25 MAT microscope and Image Pro-Analyzer software are employed to accurately quantify porosity. The combination of experimental data with statistical modeling enables the formulation of a regression-based mathematical model that predicts average coating porosity as a function of the three primary technological parameters [15].

The urgency of this research lies in its potential to support more consistent and optimized plasma coating procedures, especially for applications demanding high reliability and resistance to wear and corrosion. The main contribution of this study is the development of an empirical porosity model that can guide process optimization and serve as a decision-making tool for engineers and materials scientists. In practical terms, the model enables better control

https://doi.org/10.12928/spekta.v6i1.10985

over coating microstructure, enhancing performance and service life of mechanical components in challenging operational environments.

Accordingly, the research is guided by the following problem formulation: How do variations in plasma spray distance (Lp), current intensity (Ip), and powder feed flow rate (Gp) influence the average porosity of Al_2O_3–TiO_2 ceramic coatings on carbon steel substrates? The objective of this study is to construct a predictive and statistically reliable model that links these parameters to coating porosity, thereby enabling improved process control and material design for surface engineering applications.

2. Method

This study employed a quantitative experimental research design aimed at modeling the relationship between plasma spraying process parameters and the resulting porosity of ceramic coatings. The experimental procedure was conducted under controlled laboratory conditions using a standardized orthogonal experimental design to ensure reliability and reproducibility of results [11], [12].

The substrate material used in the experiment was SS400 carbon steel, fabricated into disc-shaped specimens with a diameter of 50 mm and a thickness of 3 mm. Plasma coatings were applied directly to the surface of these specimens without any intermediate bonding layer. The coating material consisted of a commercially available ceramic alloy powder composed of Al_2O_3 with 40% TiO_2. Plasma spraying was performed using a Model 3710 - 40 kW plasma spraying system at the Key Laboratory of Welding and Surface Treatment Technology, National Institute of Mechanical Engineering. Spraying was carried out in atmospheric conditions with natural air cooling in a normalized mode immediately after the deposition process [11].

The experimental design followed an extended orthogonal array of type $N = 3^3 = 27$, which enabled the systematic variation of three critical process parameters: spray distance (Lp), plasma current intensity (Ip), and powder feed rate (Gp). Each of the 27 experiments represented a unique combination of these parameters within the operational range recommended by the equipment manufacturer. Data on coating porosity were obtained from metallographic examination of cross-sectional samples. After spraying, the coated specimens were sectioned, polished, and analyzed using the Axiovert 25 MAT optical microscope integrated with Image Pro-Analyzer software [10], [16]. Porosity values were measured based on digital image analysis techniques, which involved quantifying the percentage of voids relative to the total coating area. This approach allowed for a detailed assessment of microstructural integrity across all test conditions [17].

The primary data source consisted of the porosity values (in percentage) derived from each of the 27 experimental conditions. All measurements were repeated to ensure consistency, and average values were calculated to represent each test point. Statistical analysis was performed using empirical modeling and regression techniques based on the least square method. The

experimental data were processed using specialized software such as MATLAB and Statistic, which enabled the development of a polynomial regression model linking Lp, Ip, and Gp to the average porosity (γ). This mathematical model serves as a predictive tool for estimating porosity under varying spray conditions.

To ensure the validity and reliability of the data, multiple strategies were employed. Each experimental run was performed under standardized conditions with careful calibration of the plasma equipment prior to spraying. Repeated porosity measurements were taken from multiple cross-sections of each sample to minimize measurement error. Statistical deviation (S^2) between observed and modeled porosity values was calculated to assess the accuracy of the model. Acceptable error margins, based on engineering standards for porosity modeling, were used to validate the predictive capability of the regression equation.

In summary, the study integrates a structured experimental approach with quantitative data analysis to derive a robust model for predicting porosity in plasma-sprayed ceramic coatings. The combination of orthogonal design methodology, high-resolution image analysis, and statistical modeling ensures a high level of confidence in the results and their applicability in industrial coating processes, as seen in Figure 1.

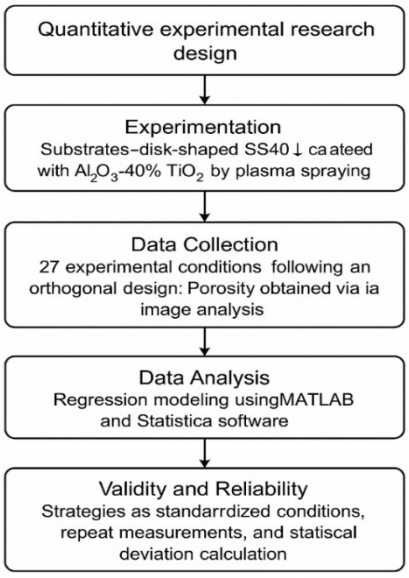

Figure 1. Flowchart Method

3. Results and Discussion

3.1. Results

The parameters of plasma coating spraying technology from Al2O3+ 40% TiO2 commercial spray powder selected for investigation in 27 experiments include: Spray distance: Lp = 100 (200 mm; Ip plasma current strength = 400 (600 A; Gp spray feed flow = 1.7 (2.1 kg/h and spray speed Vp = 50 mm/min; Primary air supply flow Ar: 150 l/min, secondary gas N2: 15 l/min, transport gas Ar: 15 l/min; spray sample temperature: 100 (150°C; natural cooling in air. The

https://doi.org/10.12928/spekta.v6i1.10985

results of experiments and mathematical model calculations of the average porosity of plasma coating materials are given in Table 1.

Table 1. Plan experiment

Mark	Code	Spray distance LP, mm	Current of plasma, IP, A	Spray feed flow, GP, kg/min	Average porosity of plasma coating, ◎, %		
					Experiment,◎ t.n	Calculation, ◎ t.t	Deviation (S^2)
1	000	100	400	1,7	14,520	14,675	+ 1,07
2	010	100	500	1,7	13,538	12,88	◎ 4,86
3	020	100	600	1,7	11,355	11,125	◎ 2,02
4	100	150	400	1,7	10,985	11,159	+ 1,59
5	110	150	500	1,7	9,695	10,111	+ 4,29
6	120	150	600	1,7	7,765	8,8491	+ 13,96
7	200	200	400	1,7	8,125	8,2424	+ 1,44
8	210	200	500	1,7	7,773	7,6868	◎ 1,11
9	220	200	600	1,7	7,321	6,9176	◎ 5,51
10	001	100	400	1,9	11,524	11,807	+ 2,45
11	011	100	500	1,9	10,350	10,532	+ 1,75
12	021	100	600	1,9	9,153	9,0429	◎ 1,20
13	101	150	400	1,9	8,465	8,9166	+ 5,33
14	111	150	500	1,9	7,566	7,9851	+ 5,54
15	121	150	600	1,9	6,676	6,8399	+ 2,46
16	201	200	400	1,9	6,976	6,3712	◎ 8,67
17	211	200	500	1,9	6,026	5,7832	◎ 4,03
18	221	200	600	1,9	5,060	4,9816	◎ 1,54
19	002	100	400	2,1	12,485	11,894	◎ 4,74
20	012	100	500	2,1	11,058	10,884	◎ 1,57
21	022	100	600	2,1	9,950	9,6613	◎ 2,90
22	102	150	400	2,1	8,774	9,3748	+ 6,85
23	112	150	500	2,1	7,850	8,5599	+ 9,04
24	122	150	600	2,1	6,976	7,5315	+ 7,97
25	202	200	400	2,1	7,250	7,2008	◎ 0,68
26	212	200	500	2,1	6,676	6,5804	◎ 1,43
27	222	200	600	2,1	5,955	5,7464	◎ 3,50

The calculation of hidden coefficients by the method of least squares in a higher-order general mathematical model representing the target function to be found in the selected survey domain for 27 different plasma injection experimental modes can be performed according to the orthogonal experimental matrix algorithm given in the works [18] and [19] when

considering copper influences The timing of the 3 main technological parameters of plasma injection is stated. However, currently some computer software handles empirical mathematical statistics for most basic studies such as Statistic lab, it is also possible to produce 2D and 3D graphs along with corresponding numerical models when considering the simultaneous pairing influence of 2 of the 3 selected technological parameters on the output target function is quite reliable.

Figure 2 is the result of a 3D graph construction calculation showing the dependence of the average porosity of the Al2O3+ 40% TiO2 plasma coating on the pair of Ip injection technology parameters. Gp; and Figure 3, couple Lp. Ip and Figure 4, couple Lp. Gp.

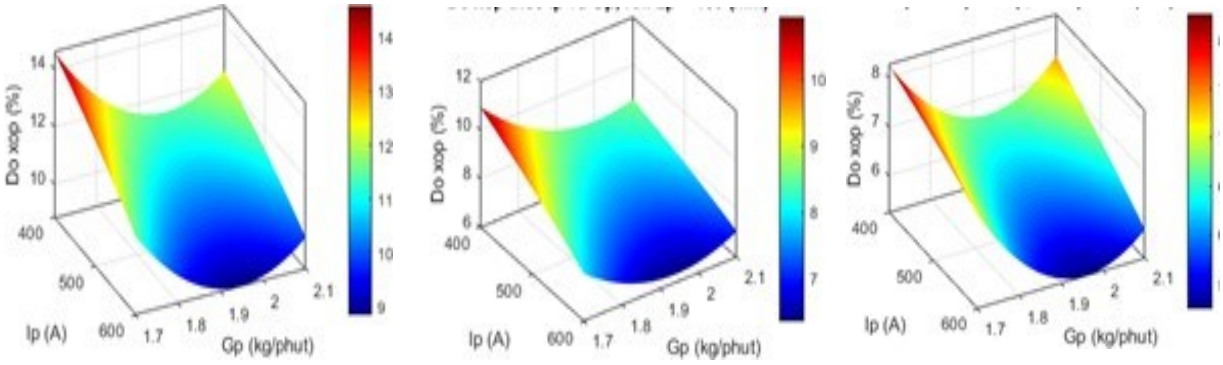

a) LP = 100 mm b) LP = 150 mm c) LP = 200 mm

Figure 2. Simultaneous influence pairing of Ip spray parameters. Gp to medium porosity Ceramic alloy plasma coating Al2O3+ 40% TiO2 when Lp changes (Vp = 50 mm/s)

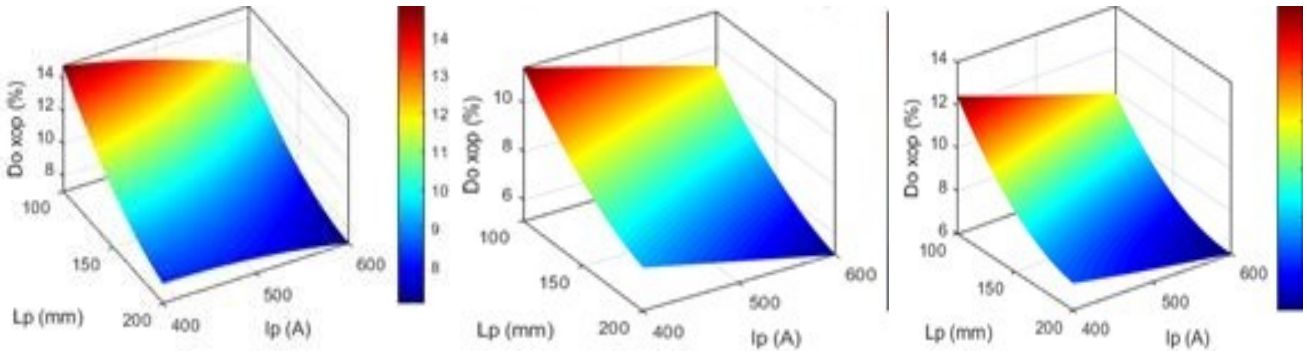

a) GP = 1,7 kg/h b) GP = 1,9 kg/h c) GP = 2,1 kg/h

Figure 3. Simultaneous influence pairing of Lp spray parameters. Ip to medium porosity Ceramic alloy plasma coating Al2O3+ 40% TiO2 when Gp changes (Vp = 50 mm/s)

The results of interpolation analysis in the change domain of 3 plasma injection technology parameters at the average adjustment levels according to the N27 experimental plan correspond to the following conditions: Ip = 500 A (Figure. 4, b); Lp = 150 mm (Figure 2, b); Gp =1.9 kg/h (Figure 3, a); Lp = 150 mm (Figure 2, b); Gp = 1.9 kg/h (Figure 3, a) and Ip = 500 A (Figure 4, b).

https://doi.org/10.12928/spekta.v6i1.10985

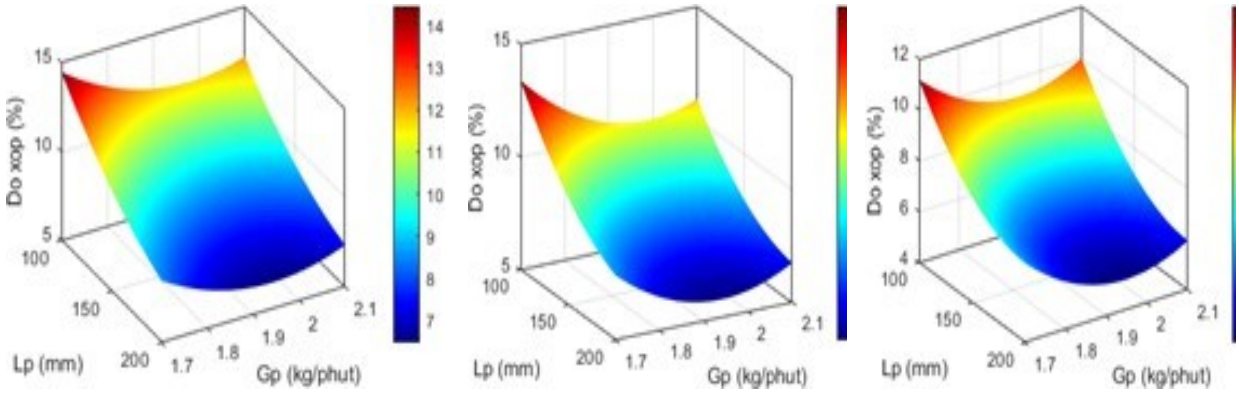

a) IP = 400 A b) IP = 500 A c) IP = 600 A

Figure 4. Simultaneous influence pairing of Lp spray parameters. Gp to medium porosity Ceramic alloy plasma coating Al2O3+ 40% TiO2 when Ip changes (Vp = 50 mm/s).

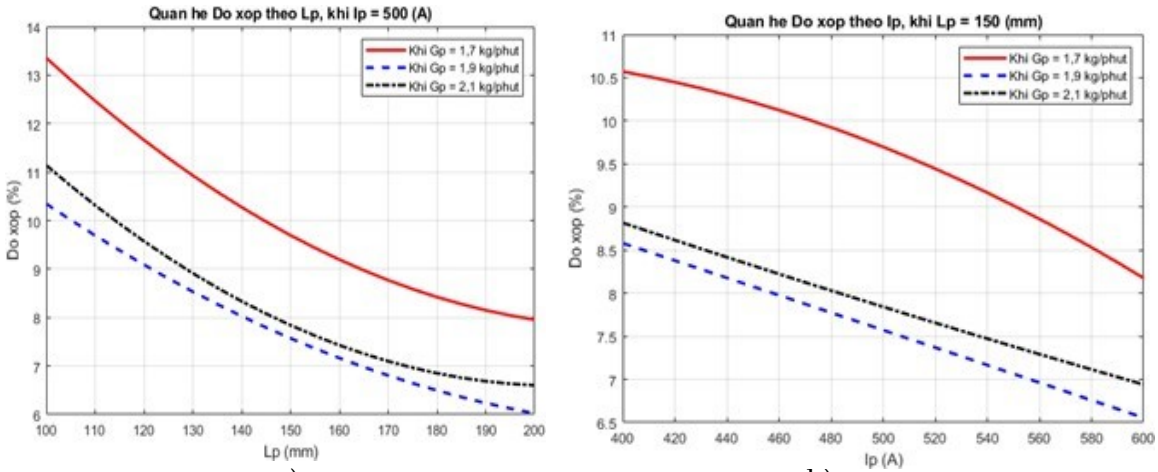

a) b)

Figure 5. The dependence of average porosity of Al2O3+ 40% TiO2 plasma coating on Lp spray distance when Ip = 500 A (a) and Ip plasma flow strength when Lp = 150 mm (b); Vp = 50 mm/s.

This study investigated the effect of three principal plasma spraying parameters, spray distance (Lp), plasma current intensity (Ip), and powder feed rate (Gp), on the average porosity of Al_2O_3 + 40% TiO_2 ceramic coatings applied to SS400 carbon steel substrates. The experiments were carried out under 27 different spray mode combinations, following an N27 orthogonal experimental matrix. The parameter ranges used were: Lp from 100 to 200 mm, Ip from 400 to 600 A, and Gp from 1.7 to 2.1 kg/h, with a constant spray speed (Vp) of 50 mm/min. All samples were sprayed in an atmospheric environment and subsequently cooled in ambient air without additional post-treatment.

The resulting porosity data obtained through image analysis were compared with predicted values calculated using a higher-order regression model developed through the least square method. The model equation is as follows:

This regression model describes the nonlinear interaction of the three input variables and enables the prediction of coating porosity under various parameter combinations. A comparison between experimental and predicted porosity values is presented in Table 1. The calculated deviations (S^2) ranged from −8.67% to +13.96%, demonstrating a generally acceptable level of accuracy for empirical modeling in thermal spray research.

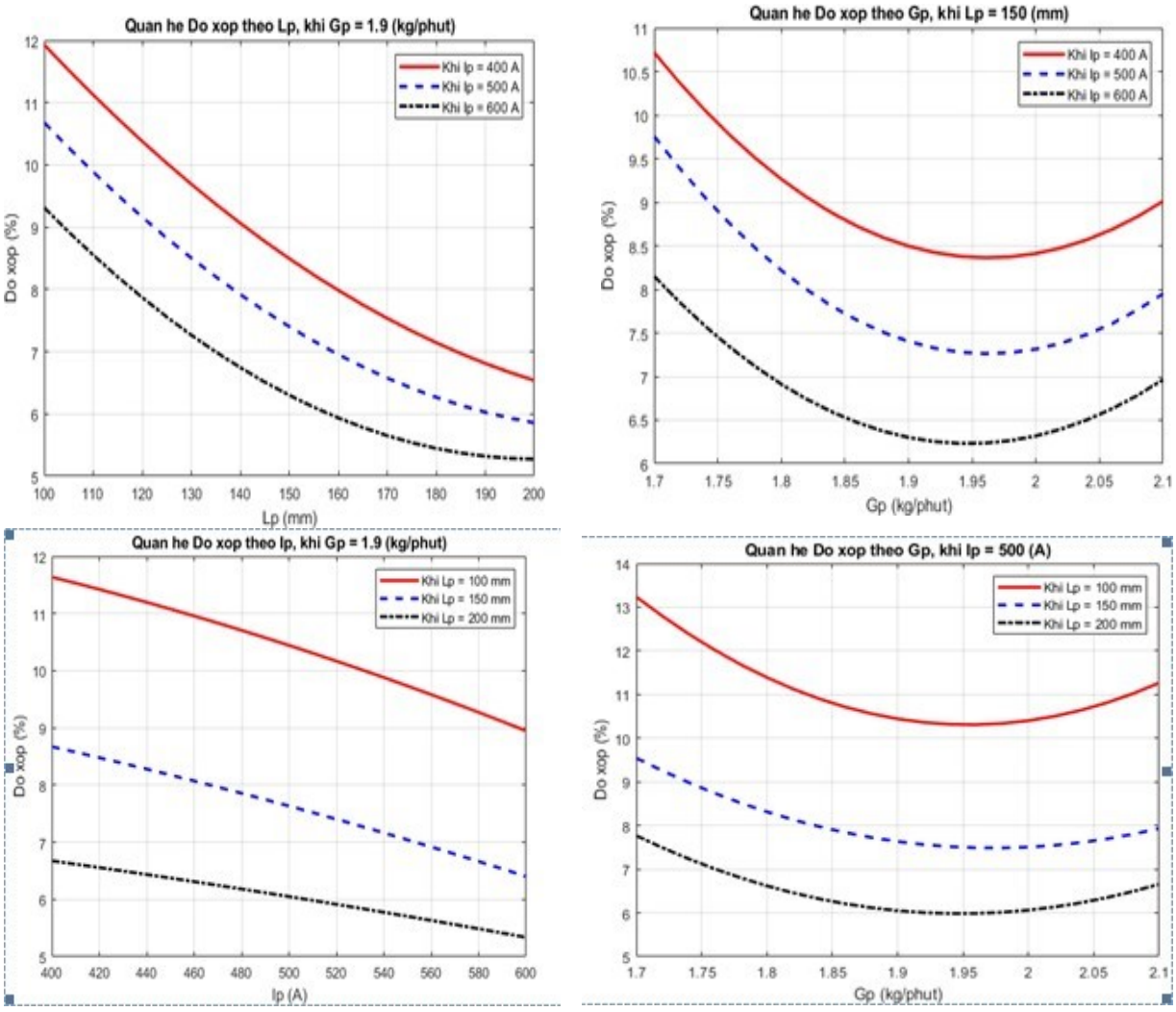

a) b)

Figure 6. The dependence of the average porosity of the Al2O3+ 40% TiO2 plasma coating on the Ip plasma flow strength when Gp = 1.9 kg/h (a) and the spray powder feed flow Gp when Ip =500 A (b); Vp = 50 mm/s.

The analysis of the results reveals that porosity tends to decrease with increasing plasma current and feed rate, particularly at lower spray distances. For instance, when Lp was fixed at 100 mm and Gp at 1.7 kg/h, increasing Ip from 400 A to 600 A resulted in a porosity reduction from 14.52% to 11.36%. Similar trends were observed across other parameter combinations. This inverse relationship aligns with established principles in plasma spray processing, where

https://doi.org/10.12928/spekta.v6i1.10985

higher current and feed rate improve particle melting and impact velocity, thereby reducing void formation upon deposition.

3D response surface plots were generated to visualize the interactive influence of parameter pairs Figure 3, Figure 4 and Figure 5. Figure 3 shows the combined effect of Ip and Gp on porosity for different Lp values. At Lp = 100 mm, increasing either Ip or Gp consistently reduced porosity. However, at Lp = 200 mm, the trend reverses slightly due to the loss of thermal energy and particle velocity before reaching the substrate. Figure 4 illustrates how Lp and Ip affect porosity at fixed Gp values, revealing that moderate spray distances (150 mm) with high current yield optimal porosity values. Similarly, Figure 5 demonstrates that the combination of shorter spray distance (Lp) and higher feed rate (Gp) contributes to lower porosity when Ip is sufficiently high.

Further interpolation analysis was conducted at mid-range parameter settings: Ip = 500 A, Lp = 150 mm, and Gp = 1.9 kg/h. The results Figure 5, Figure 6 confirmed the nonlinear behavior of porosity with respect to individual parameters. Specifically, at constant Ip = 500 A, increasing Lp beyond 150 mm resulted in a slight increase in porosity, indicating a threshold beyond which spray distance negatively impacts deposition quality. Conversely, at fixed Lp = 150 mm, increasing Gp showed an initial porosity reduction followed by a slight increase, suggesting an optimal powder feed rate around 1.9 kg/h.

Overall, the results indicate that porosity in plasma-sprayed Al_2O_3–TiO_2 coatings can be effectively controlled by tuning the key spray parameters within a defined operational window. The derived regression model provides a reliable tool for predicting porosity levels based on parameter inputs and can serve as a reference for optimizing plasma spray processes in industrial applications. The analysis also underscores the importance of understanding multivariable interactions in thermal spray systems, which are often overlooked in traditional single-variable studies.

3.2. Discussion

The experimental results and modeling efforts presented in this study aim to address the research problem formulated as follows: How do variations in plasma spray parameters, specifically spray distance (Lp), plasma current (Ip), and powder feed rate (Gp), influence the average porosity of Al_2O_3 + 40% TiO_2 ceramic coatings on SS400 carbon steel substrates? The goal was to develop a statistically valid and predictive model that captures the nonlinear relationships among these parameters and their effects on coating quality, particularly porosity.

This study is grounded in the theoretical framework of plasma heat and momentum transfer and particulate deposition dynamics, which suggest that the porosity of thermally sprayed ceramic coatings is primarily influenced by particle melting efficiency, velocity, and adhesion upon substrate impact. According to thermal spray theory, higher plasma arc currents (Ip) increase the energy input into the system, enabling more complete melting of

particles, thereby reducing porosity. Similarly, optimal spray distance (Lp) ensures sufficient particle velocity and temperature at the substrate, while an appropriate powder feed rate (Gp) avoids under- or over-saturation of particles in the plasma jet [20].

In practice, these theoretical principles are subject to complex interactions, and as such, an orthogonal experimental design (N27) was employed to systematically explore these variables. The empirical data confirm the theoretical expectations: increasing plasma current consistently reduced porosity, especially at shorter spray distances and moderate feed rates. This behavior was evident in all three orthogonal sub-arrays (N9(1), N9(2), and N9(3)), validating the role of Ip in enhancing particle melting and impact quality.

For instance, in the N9(1) group (Gp = 1.7 kg/h), the porosity decreased from 14.52% to 11.36% as Ip increased from 400 A to 600 A at Lp = 100 mm. The reduction trend continued in the N9(2) and N9(3) sets, with the lowest porosity (5.96%) observed at Lp = 200 mm, Ip = 600 A, and Gp = 2.1 kg/h. However, it is also evident that excessively long spray distances led to increased porosity in certain conditions, consistent with theoretical concerns over particle cooling and deceleration before impact.

The empirical regression model derived in this study encapsulates these findings into a second-order polynomial equation, which effectively quantifies the contribution of individual parameters and their interactions. The model's reliability is demonstrated through the error margin (S^2), which in most cases remains within acceptable limits for engineering applications. These findings directly support the objective of the study, namely: to construct a predictive model that enables control of coating porosity through appropriate selection of process parameters [21]–[23].

Further insights are obtained from the 3D surface response graphs. These reveal that while each parameter individually influences porosity, their interactions often determine the final coating structure [24]. The graphs show that optimal coating densification occurs at moderate spray distances (150 mm), high plasma currents (500–600 A), and feed rates around 1.9 kg/h. These results align with theoretical expectations from plasma-particle interaction models, such as those developed in heat transfer and two-phase flow analyses of the plasma spray process [25], [26].

The 2D interpolation graphs Figure 4, Figure 5, and Figure 6 confirm the non-linear but smooth dependency of porosity on input parameters. These relationships indicate that while trends are predictable, they are not strictly linear, requiring multivariable modeling for accurate control. The slight increase in porosity observed beyond certain Gp thresholds (e.g., 1.9 kg/h to 2.1 kg/h) is attributed to particle agglomeration or oversaturation, which is a well-documented phenomenon in high-feed-rate plasma spraying [27], [28].

In connecting back to the research background, this study fills an important gap where many previous works lacked statistical depth or comprehensive modeling of parameter interactions. The current research advances both the theoretical understanding and practical

https://doi.org/10.12928/spekta.v6i1.10985

control of ceramic plasma coatings, particularly for applications demanding high performance, such as in wear-resistant and thermally stressed components [29], [30].

In conclusion, the research effectively answers the central research question by demonstrating how the process parameters influence porosity and by providing a predictive model to guide parameter optimization. This study not only confirms known theoretical principles but also provides a validated empirical framework that can be directly applied in surface engineering practices, contributing to both academic knowledge and industrial advancement.

4. Conclusion

This study successfully developed a predictive mathematical model linking spray distance, plasma current intensity, and powder feed rate to the porosity level of Al_2O_3 + 40% TiO_2 ceramic coatings on SS400 substrates. The model demonstrated good accuracy, with deviations mostly within ±9%, validating its reliability for optimizing plasma spray parameters to meet specific porosity requirements.

Despite being limited to a narrow parameter range and a single material system, the model provides a practical tool for process control in thermal spray applications. Future research should explore broader parameter domains, additional material systems, and the influence of post-treatment processes to enhance model applicability and performance prediction in real-world industrial settings.

Acknowledgment

This research has not received external funding.

References

[1] G. Yang, B. Fu, T. Dong, and G. Li, "Preparation of AlSi30Cu5 coating with fine microstructure using plasma spraying technology," *Mater. Lett.*, 2024, [Online]. Available: https://www.sciencedirect.com/science/article/pii/S0167577X23019857.

[2] X. Li, "Effect of TiO2 content on the thermal control properties of Al2O3-xTiO2 composite coatings prepared by supersonic plasma spraying technology," *Journal of Materials Research and Technology*. Elsevier, 2024, [Online]. Available: https://www.sciencedirect.com/science/article/pii/S2238785424019896.

[3] S. Zhu, "Ablation behavior and mechanisms of high-entropy rare earth titanates (Y0. 2Gd0. 2Ho0. 2Er0. 2Yb0. 2) 2Ti2O7 coating deposited by plasma spraying technology," *Surface and Coatings Technol.*, 2024, [Online]. Available: https://www.sciencedirect.com/science/article/pii/S0257897224000446.

[4] C. Cheng, "Thermal cycling property of the novel Hf6Ta2O17/YSZ TBCs prepared by

atmospheric plasma spraying technology," *Surfaces and Interface*, 2024, [Online]. Available: https://www.sciencedirect.com/science/article/pii/S2468023024012069.

[5] P. Daram, Y. Morisada, T. Ogura, M. Kusano, and J. Yu, "Development of Tungsten Repair Technology by Atmospheric Plasma Spraying of Tungsten and Friction Stir Processing," *Journal of Thermal Spray Technol.*, 2024, doi: 10.1007/s11666-024-01820-5.

[6] V. I. Kolesnikov, O. V Kudryakov, V. N. Varavka, I. V. Kolesnikov and K. N. Polityko, "Self-Organizing Processes in the Structure of CrTiZrNbHf (HEA) Ion-Plasma Coatings Obtained Using a Multicathode Arc Spraying Technology," *J. Mach. Manufacture and Reliability*, 2024, doi: 10.1134/S105261882470122X.

[7] K. Khanlari, I. E. Achouri, and F. Gitzhofer, "Exploring thermal-plasma spraying technology for advanced aluminum-based materials," *Powder Technol.*, 2023, [Online]. Available: https://www.sciencedirect.com/science/article/pii/S0032591023005193.

[8] O. G. Devoino, A. V Gorbunov, A. S. Volodko, and A. N. Polyakov, "Investigation of upgraded technology for plasma spraying of bronze powder using the combined process with hydrocarbon additions," *Belarusian National Technical University*. cyberleninka.ru, 2023, [Online]. Available: https://cyberleninka.ru/article/n/investigation-of-upgraded-technology-for-plasma-spraying-of-bronze-powder-using-the-combined-process-with-hydrocarbon-additions.

[9] B. N. Guzanov, N. B. Pugacheva, E. Y. Slukin, and T. M. Bykova, "Technology of obtaining composite conglomerate powders for plasma spraying of high-temperature protective coatings," *Obrabotka metallov*. 2021. Doi: 10.17212/1994-6309-2021-23.1-6-20

[10] R. Wang, "Low-pressure plasma spraying of ZrB2–SiC coatings on C/C substrate by adding TaSi2. Surface &Coa tings Technology. 2021; 420: 127332." 2021. Doi: 10.1016/j.surfcoat.2021.127332

[11] G. Zheng, T. Xiong, S. Yanfang, X. Cui, W. Jiqiang, T. Junrog, L. Ning, Q. Jianzhong, and T. Yongshan, "Method for preparing a protective coating on a surface of key components and parts of IC devices based on plasma spraying technology and cold spraying technology," *US Pat. Google*, 2023, [Online]. Available: https://patents.google.com/patent/US11834748B2/en.

[12] N. X. Cuong, "*Research on plasma spraying technology for fabrication of silicon carbide plasma coating on steel surface to protect against corrosion in the fluorine*." Ministry of Industry and Trade, Hanoi, 2023.

[13] M. I. Boulos, P. L. Fauchais, and J. V. R. Heberlein, "DC Plasma Spraying, Process Technology," *Thermal Spray Fundamentals From Powder to Part*, 2021, doi: 10.1007/978-3-030-70672-2_9.

[14] P. Derevyankin and V. Frolov, "Analysis of the transient contact resistance of composite copper-graphite material obtained using plasma spraying technology," *Mater. Sci.*

https://doi.org/10.12928/spekta.v6i1.10985

Forum, 2021, [Online]. Available: https://www.scientific.net/MSF.1022.27.

[15] V. S. Bessmertnyi, N. M. Zdorenko, V. M. Vorontsov, and M. A. Bondarenko, "Energy-Saving Technology of Assorted Glassware Decoration by Plasma Spraying," *Glas. Ceram.*, 2022, doi: 10.1007/s10717-022-00411-6.

[16] P. G. Derevyankin and V. Y. Frolov, "Analysis of erosion processes of electrical contacts manufactured by plasma spraying technology," *2020 IEEE Conf. of Russian Young Researchers in Electrial and Electronic Engineering*, 2020, [Online]. Available: https://ieeexplore.ieee.org/abstract/document/9039012/.

[17] V. I. Kalita, D. A. Malanin, A. I. Mamaev, V. A. Mamaeva, and V. V. Novochadov, "Plasma spraying for additive preparation technology of 3D bioactive coatings with a new type of porous ridge/cavity structure," *Cavity AMI: Materialia*, 2020, [Online]. Available: https://papers.ssrn.com/sol3/papers.cfm?abstract_id=3702819.

[18] Y. Zhiguts, V. Lazar, and B. Khomiak, "Fitments for technology of SHS and plasma spraying." dspace-s.msu.edu.ua, 2020, [Online]. Available: http://dspace-s.msu.edu.ua:8080/bitstream/123456789/6588/1/Fitments_for_technology_of_SHS_and_plasma_spraying.pdf.

[19] J. Xu, J. Lee, and Y. Shao, "Direct write plasma spraying technology applied to the semiconductor industry," *US Pat. App. 16/631,216*, 2020, [Online]. Available: https://patents.google.com/patent/US20200140987A1/en.

[20] M. Hong, "Low pressure plasma spraying technology and research status," *Precision Forming*. 2020.

[21] M. Shi, Z. Xue, Z. Zhang, X. Ji, E. Byon, and S. Zhang, "Effect of spraying powder characteristics on mechanical and thermal shock properties of plasma-sprayed YSZ thermal barrier coating," *Surf and Coat Technol*. 2020. https://www.sciencedirect.com/science/article/abs/pii/S025789722030582X

[22] A. A. Kovalev and A. S. Krasko, "Problems of the application of supersonic plasma spraying in the conditions of small-batch production,(Modern Materials, Technics, and Technology)." Yugo-Zapadnyi Gos. Univ., 2020.

[23] J. Chen, J. Xiao, H. Tan, Y. Wu, J. Chen, and C. Zhang, "Microstructure and Wear Behavior of FeCoNiCrMn High Entropy Alloy Coating Deposited by Plasma Spraying," *Surf. Coat. Technol.* 2020. https://www.sciencedirect.com/science/article/abs/pii/S0257897220300992

[24] R. Musalek, J. Medricky, J. Kotlan, T. Tesar, Z. Pala, F. Lukac, and T. Chraska, "Plasma Spraying of Suspensions with Hybrid Water-Stabilized Plasma Technology," *Int. Thermal Spray Conference*, 2016, [Online]. Available: https://dl.asminternational.org/itsc/proceedings-abstract/ITSC2016/83768/267/26112.

[25] S. S. Dautov, P. G. Shornikov, L. R. Rezyapova, and I. S. Akhatov, "Increasing thermal

and mechanical properties of thermal barrier coatings by suspension plasma spraying technology," *J. Phys. Conferences Series*, 2019, doi: 10.1088/1742-6596/1281/1/012008.

[26] Z. Wang, L. Z. Du, H. Lan, C. B. Huang, and W. G. Zhang, "A novel technology of Sol precursor plasma spraying to obtain the ceramic matrix abradable sealing coating," *Mater. Lett.*, 2019, [Online]. Available: https://www.sciencedirect.com/science/article/pii/S0167577X19307918.

[27] I. P. Grishina, S. V Telegin, A. V Lyasnikova, O. A. Markelova, and O. A. Dudareva, "Development of the combined technology of modification of the surface of titanium implants by laser radiation with subsequent plasma spraying of biocompatible coatings," *Metallurgist*, 2019, doi: 10.1007/s11015-019-00812-z.

[28] P. Derevyankin, V. Frolov, D. Gonzalez, S. Gortschakow, R. Methling and D. Uhrlandt, "Analysis of erosion resistance of CuC arcing contacts manufactured by plasma spraying technology," *Plasma Physics and Technol.*, 2019, [Online]. Available: https://ojs.cvut.cz/ojs/index.php/PPT/article/view/5741.

[29] S. Niu, K. Zhou, C. Deng, L. Xu, M. Liu, W. Zeng and Z. Chen, "Formation mechanism of island CoO in La-Sr-Co-Fe oxygen transport membrane deposited by low pressure plasma spraying-thin film technology," *J. Phys.: Conference Series*, 2019, doi: 10.1088/1742-6596/1347/1/012115.

[30] H. Z. Cai, H. E. Hui-Xia, and F. X. Wang, "The plasma spraying technology on titanium bases surface treatment on the effects of the human periodontal ligament stem cell growth," *Chin J Geriat Dent*. 2017.

https://doi.org/10.12928/spekta.v6i1.10985